Mayotte coral reveales hydrological changes in the western Indian between 1865 to 1994

Zinke, J.; Timm, O.; Pfeiffer, M.; Dullo, W.-C.; Kroon, D.; Thomassin, B.A.

published in
Geophysical Research Letters
2008

DOI (link to publisher)
10.1029/2008GL035634

document version
Publisher's PDF, also known as Version of record

Mayotte coral reveals hydrological changes in the western Indian Ocean between 1881 and 1994

J. Zinke,[1] M. Pfeiffer,[2] O. Timm,[3] W.-C. Dullo,[4] D. Kroon,[5] and B. A. Thomassin[6]

Received 8 August 2008; revised 22 September 2008; accepted 5 November 2008; published 10 December 2008.

[1] We reconstruct the hydrologic history of the tropical western Indian Ocean by calculating the $\delta^{18}O_{seawater}$ from coupled coral Sr/Ca and $\delta^{18}O$ measurements in a massive *Porites* coral from Mayotte (Comoros) between 1881 and 1994. We found that the precipitation-evaporation balance varies naturally on time scales of 5–6 years and 18–25 years. High (low) SSTs are associated with positive (negative) $\delta^{18}O_{seawater}$ implying that atmospheric variability is linked with remote climate modes in the Indian Ocean and the tropical/extratropical Pacific Ocean. Warm El Niño-Southern Oscillation events are associated with a negative freshwater balance at Mayotte. This case study demonstrates that a much denser network of $\delta^{18}O_{seawater}$ reconstructions is crucial for understanding the spatial patterns of hydrological conditions. **Citation:** Zinke, J., M. Pfeiffer, O. Timm, W.-C. Dullo, D. Kroon, and B. A. Thomassin (2008), Mayotte coral reveals hydrological changes in the western Indian Ocean between 1881 and 1994, *Geophys. Res. Lett.*, *35*, L23707, doi:10.1029/2008GL035634.

1. Introduction

[2] Future global warming will trigger significant changes in surface temperature and the hydrological cycle, with both combined leading to uncertain societal and environmental consequences. For the Indian Ocean and the adjacent continents the IPCC's latest AR4 projections show a large spread [*Annamalai et al.*, 2007]. Precipitation over the oceans has a complex spatial structure and often differs from trends in underlying sea surface temperature (SST) [*Kumar et al.*, 2004]. Over the western Indian Ocean, instrumental data is too sparse to investigate the rainfall/temperature response over the ocean on interannual to multidecadal time scales [*Annamalai et al.*, 1999; *Deser et al.*, 2004]. Satellite-borne rainfall measurements, which provide high spatial coverage over the oceans, are not available before 1979, a period too short to reduce the uncertainty in the trend estimates.

[3] However, the stability of the ocean-atmosphere coupling in a changing climate is important for future climate projections. Long proxy records with sufficient temporal resolution are the only alternative to assess the stability of such connections.

[4] The close link between SST and the El Niño-Southern Oscillation (ENSO) in the western Indian Ocean north of 10°S is confirmed by a number of coral records [*Charles et al.*, 1997; *Cole et al.*, 2000; *Timm et al.*, 2005; *Zinke et al.*, 2005; *Pfeiffer et al.*, 2006], while the response of the hydrological cycle is not well understood. *Pfeiffer et al.* [2006] find positive rainfall excursions during El Nino years north of 10°S. Rainfall data from southern Africa, however, suggests that El Niño events may lead to pronounced droughts south of 10°S [*Richard et al.*, 2000].

[5] In this study we investigate long-term hydrological changes over the western Indian Ocean south of 10°S using a 113 year long, bimonthly resolved record of $\delta^{18}O$ and Sr/Ca from a *Porites solida* coral drilled at Mayotte (12°39′S, 45°06′E; Comoro Archipelago; for methodology see auxiliary materials).[1] The combination of Sr/Ca as a temperature proxy with $\delta^{18}O$ as an independent proxy for SST and $\delta^{18}O_{seawater}$ can provide simultaneous information on SST and hydrological changes [*Cahyarini et al.*, 2008, and references therein]. Our coral $\delta^{18}O_{seawater}$ series is the first of its kind from the western Indian Ocean. We will use a range of hydrological data ($\delta^{18}O_{seawater}$ and salinity measurements, rainfall and precipitation-evaporation data) collected at and around Mayotte to demonstrate that our coral proxy data can expand the current understanding of the hydrological cycle.

2. Climatic Setting of the Study Area

[6] Air Temperature (AT) and rainfall for Mayotte are available between 1949 to present and 1933 to present, respectively (NOAA GHCN monthly Weather Station at Pamandzi/Dzaoudzi, 12.80°S, 45.28°E). An inferred local SST record (hereafter SSTi) back until 1949 is derived from linear regression of *in-situ* lagoonal SST with local air temperature for the calibration period 1999–2002 (equation: SST = 0.8535*AT + 4.7733; r^2 = 0.85). Regional precipitation minus evaporation (P-E) and outgoing longwave radiation (OLR) data are taken from NCEP/NCAR reanalysis [*Kalnay et al.*, 1996] averaged over 10–15°S, 40–45°E. Monthly gridded sea level pressure (SLP) data are taken from the Met Office of the Hadley Centre of the UK [*Allan and Ansell*, 2007].

[7] SST and rainfall show an unimodal distribution with highest temperatures and rainfall between December to April (Figure S1). We investigated the relationship between

[1]Paleoclimatology and Geomorphology, Vrije Universiteit Amsterdam, Amsterdam, Netherlands.
[2]Institut für Geologie und Mineralogie, Universität zu Köln, Cologne, Germany.
[3]IPRC, SOEST, University of Hawaii, Honolulu, Hawaii, USA.
[4]Department of Ocean Circulation and Climate, Leibniz Institut fuer Meereswissenschaften, IFM-GEOMAR, Kiel, Germany.
[5]School of GeoSciences, University of Edinburgh, Edinburgh, UK.
[6]Station marine d'Endoume, Centre d'Oceanologie de Marseille, Marseille, France.

0094-8276/08/2008GL035634$05.00

[1]Auxiliary materials are available in the HTML. doi:10.1029/2008GL035634.

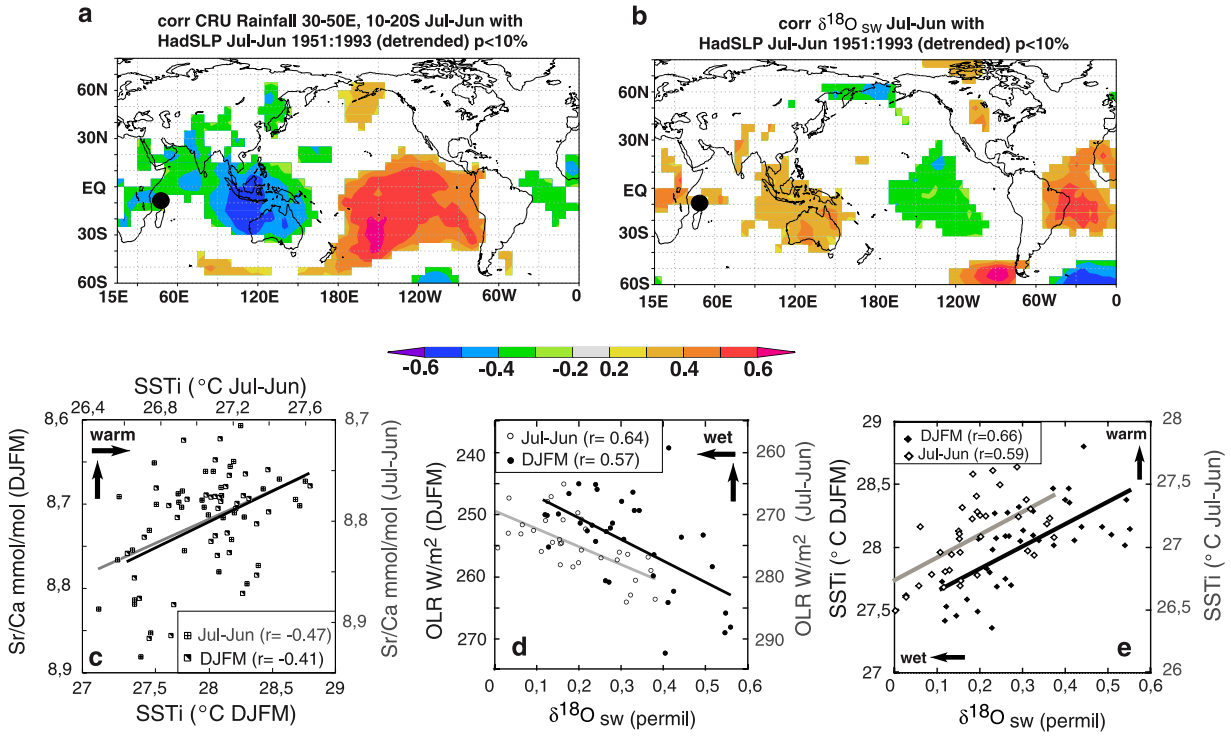

Figure 1. Spatial correlation of mean annual averages (July to June) of (a) rainfall data averaged between 30–50°E and 10–20°S including Mayotte (black circle) and (b) of $\delta^{18}O_{seawater}$ ($\delta^{18}O_{sw}$) with gridded sea level pressure (HadSLP) [*Allan and Ansell*, 2007]. Shading represents confidence of 90% and greater. Red shading indicates positive correlations and blue negative correlations. (c) Linear regression between mean annual and December to March averaged Sr/Ca ratios with local sea surface temperatures, (d) same as in Figure 1c but for $\delta^{18}O_{seawater}$ ($\delta^{18}O_{sw}$) with outgoing longwave radiation (OLR) [*Kalnay et al.*, 1996] for the period 1958 to 1993 and (e) same as in Figure 1d but for local sea surface temperatures. Correlation coefficients are indicated. Correlations are significant at the 5% level.

(i) annual mean regional rainfall in the region of Mayotte (averaged between 30–50°E, 10–20°S) and the global SLP field (Figure 1a), and (ii) seasonal mean (December–March, hereafter DJFM) AT/SSTi from Mayotte with the global SST field between 1951 and 1993 (Figure S2). The correlation maps indicate the typical global ENSO SLP (Figure 1a) and SST (Figure S2) pattern. At Mayotte, negative rainfall and positive SST anomalies occur during El Niño events (Table S1).

3. Local Hydrology and Seawater Oxygen Isotopic Variations

[8] In the Mayotte region $\delta^{18}O_{seawater}$ is modified by (i) rainout of isotopically depleted rainfall from warm air masses over deep convective regions (the so-called amount effect [*Dansgaard*, 1964]) during the intense rainy season, (ii) isotopic fractionation during evaporation and (iii) freshwater surface runoff.

[9] A detailed hydrological study at Mayotte for 1993 (dry year) versus 1994 (normal year) revealed that evaporation contributed 45–60% to the annual freshwater balance and was 15% higher under drier conditions in 1993 (Figure S3) [see also *Lapègue*, 1999]. For the given example years, evaporation contributes significantly to $\delta^{18}O_{seawater}$. The NCEP/NCAR reanalysis data for Mayotte further indicates that evaporation intra/interannual variability is of the same order as the precipitation variability.

[10] We monitored $\delta^{18}O_{seawater}$ for several months during the dry and wet season in 2002 and between September 2004 and August 2005 (Figure S3). Our $\delta^{18}O_{seawater}$ shows a maximum seasonal amplitude of 1.13‰, ranging between 0.26‰ and 1.38‰. The cause of the high values in September and October 2004 is unknown since we lack salinity data. The maximum $\delta^{18}O_{seawater}$ amplitude is reduced to 0.51‰ when September and October 2004 are not considered. The negative $\delta^{18}O_{seawater}$ values observed between August and October 2002 are related to low salinities in the lagoon (Figure S3). River runoff shows considerable interannual variability and this runoff may potentially influence $\delta^{18}O_{seawater}$ in the Mayotte lagoon (Figure S1). For 2002, minimum salinity in the lagoon lags maximum river flow by 1 month (Figure S3). This implies that the integral effect of P-E over the length of the intense rainy season and freshwater runoff into the lagoon of Mayotte resulted in a strong signal in $\delta^{18}O_{seawater}$ that persists into austral winter of 2002.

4. Results and Discussion

4.1. Calibration, Calculation of $\delta^{18}O_{seawater}$ and Error Estimates

[11] Bimonthly coral Sr/Ca ratios primarily reflect SST; linear regression yields a slope value of −0.058 mmol/mol per 1°C in agreement with published relationships [*Corrége*, 2006]. Mean annual Sr/Ca ratios show a statistically signif-

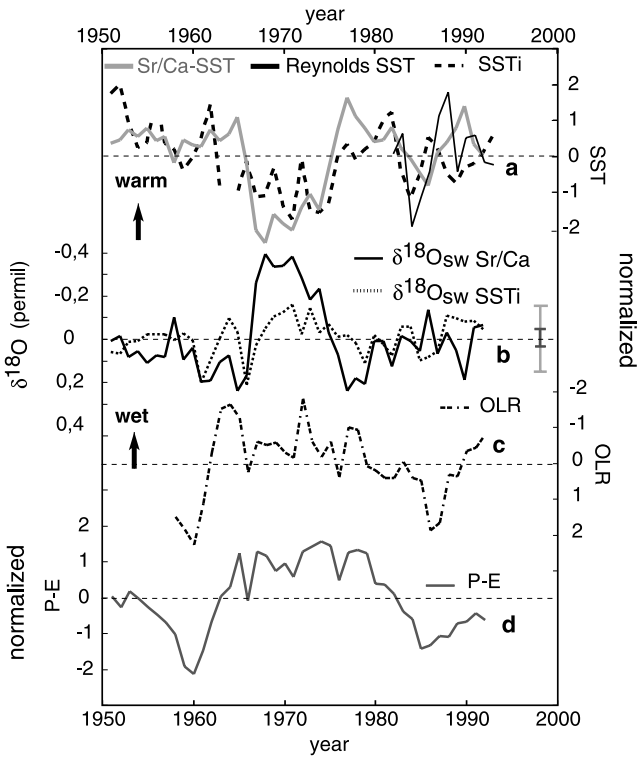

Figure 2. (a) Inferrerd SST = SSTi (dashed line; σ_{Ti} = 0.38°), grid-SST (thin line [*Reynolds et al.*, 2002]; σ_{ERSST} = 0.25°C) and Sr/Ca-SST (thick grey line; $\sigma_{Sr/Ca\text{-}SST}$ = 0.8°C). (b) Annual mean reconstructed of $\delta^{18}O_{seawater}$ ($\delta^{18}O_{sw}$) from relative changes in SSTi (stippled line) and Sr/Ca-SST (thick bold line) compared to c) OLR (dash-dotted line) and (d) precipitation minus evaporation (P-E; thick grey line) taken from NCEP/NCAR reanalysis [*Kalnay et al.*, 1996]. The 1-sigma errors for $\delta^{18}O_{seawater}$ based on the analytical error (0.037‰) and the Sr/Ca-SST mean annual regression (r = −0.47; 0.13‰) are indicated in Figure 2b. SST, OLR and P-E time series were normalized.

icant correlation of r = −0.47 ($p < 0.003$) with SSTi for the period 1950–1994 (Figure 1c). To assess the uncertainty of the SST datasets, we correlated SSTi with various SST products (ERSST, HADISST, COADS) for the grid cell including Mayotte (annual means): r ranges between 0.5–0.6. This gives us a crude estimate of the uncertainty of the SST data: approximately 70% of the SST variability is not reproducible and may reflect noise (local climatic effects, measurement errors etc.). Given these uncertainties of SSTi (and other SST products), the correlation between SSTi and coral Sr/Ca on annual mean scales indicates that Sr/Ca is a useful temperature proxy (Figure S4).

[12] We calculated $\delta^{18}O_{seawater}$ by subtracting the thermal component from coral $\delta^{18}O$ based on (i) the relative changes in Sr/Ca-SST and (ii) the relative changes of SSTi (following *Cahyarini et al.* [2008]). Our aim is to test and evaluate our $\delta^{18}O_{seawater}$ reconstruction by using SSTi as an alternative temperature record to calculate $\delta^{18}O_{seawater}$ (Figure 2). We use a $\delta^{18}O_{coral}$-SST relationship of −0.2‰/1°C [*Juillet-Leclerc and Schmidt*, 2001] and our Sr/Ca-SST relationship of −0.058 mmol/mol per 1°C. Our $\delta^{18}O_{seawater}$ reconstruction using Sr/Ca-SST (SSTi) results in a maximum seasonal amplitude of 0.69‰ (0.44‰) and a 1σ standard deviation of 0.17‰ (0.13‰; Figure 2). This agrees well with observed $\delta^{18}O_{seawater}$ variations in the monitoring experiment.

[13] To provide error estimates for our $\delta^{18}O_{seawater}$ reconstruction, we combine two different approaches. (1) The error of $\delta^{18}O_{seawater}$ is estimated based on the analytical error of coral $\delta^{18}O$ and Sr/Ca [*Cahyarini et al.*, 2008] (Figure 2). This approach is based on the assumption that with the exception of the analytical errors, Sr/Ca is a perfect record of local SST, while $\delta^{18}O$ is a perfect record of local SST plus $\delta^{18}O_{seawater}$. For bimonthly $\delta^{18}O_{seawater}$ values, the error (1σ) is 0.09‰, for annual mean $\delta^{18}O_{seawater}$ values the error reduces to 0.036‰ (see auxiliary material). (2) We estimate the statistical error resulting from the regression of $\delta^{18}O_{seawater}$ with annual mean Sr/Ca-SSTi. This approach is based on the assumption that SSTi is a perfect record of local SST at the coral site, while Sr/Ca explains only 21% of the SST variance (based on r = −0.47 with SSTi). We obtain an 1σ error of 0.13‰, for mean annual $\delta^{18}O_{seawater}$. Note, however, that this error is based on the Sr/Ca-SSTi regression only, and we cannot repeat this exercise for coral $\delta^{18}O$ due to the lack of long $\delta^{18}O_{seawater}$ records. A combined error is obtained from the two error estimates above by using the square root of the sum of squares which results in an error of 0.16 ‰ (1σ, auxiliary material).

[14] Despite potentially large errors, our $\delta^{18}O_{seawater}$ estimates based on Sr/Ca and SSTi show consistent variations. Averaging over decadal time scales and replication of Sr/Ca and $\delta^{18}O$ measurements from multiple cores could help to reduce the uncertainty significantly in the near future.

4.2. Local Climate Interpretation of $\delta^{18}O_{seawater}$

[15] Our coral Sr/Ca and $\delta^{18}O$ records show a trend towards more negative values between 1881 and 1994, indicating a long-term increase in SST (Figures 3a and 3b). Reconstructed $\delta^{18}O_{seawater}$ shows pronounced decadal and interannual variability but no long-term trend (Figure 3c). Spectral analysis reveals periodicities ranging between 5–6 years and 18–25 years (Figure S6). Linear regression analysis of DJFM and mean annual values (Figure 1d) reveals that $\delta^{18}O_{seawater}$ shows a positive (negative) correlation with OLR (rainfall and P-E; Figure S5). For the peak rainfall season our reconstruction varies coherently with the local rainfall record between 1933 and 1993 (Figure 3d). This provides confidence that our reconstruction is robust on long time scales.

[16] The temporal changes in P-E and OLR are anticorrelated with the underlying SST (Figures 1e and S5), i.e., cooler mean SSTs are associated with higher rainfall. This is particularly clear in the 1960–1980 interval, where cooler mean SSTs are accompanied by positive (negative) P-E (OLR) anomalies (Figure 2).

[17] Consistent with this, coral Sr/Ca tends to be anticorrelated with $\delta^{18}O_{seawater}$ indicating that periods of higher SST are associated with a negative freshwater balance (Figures 3a and 3c). This is particularly clear during the early phase of the pronounced wet spell that occurred between the 1960s and 1970s (Figure 2; note that the magnitude of these excursions is larger than our error estimates). Between 1961 and 1974, mean SSTs during the rainy season (NDJF) were only 27.72°C (compared to

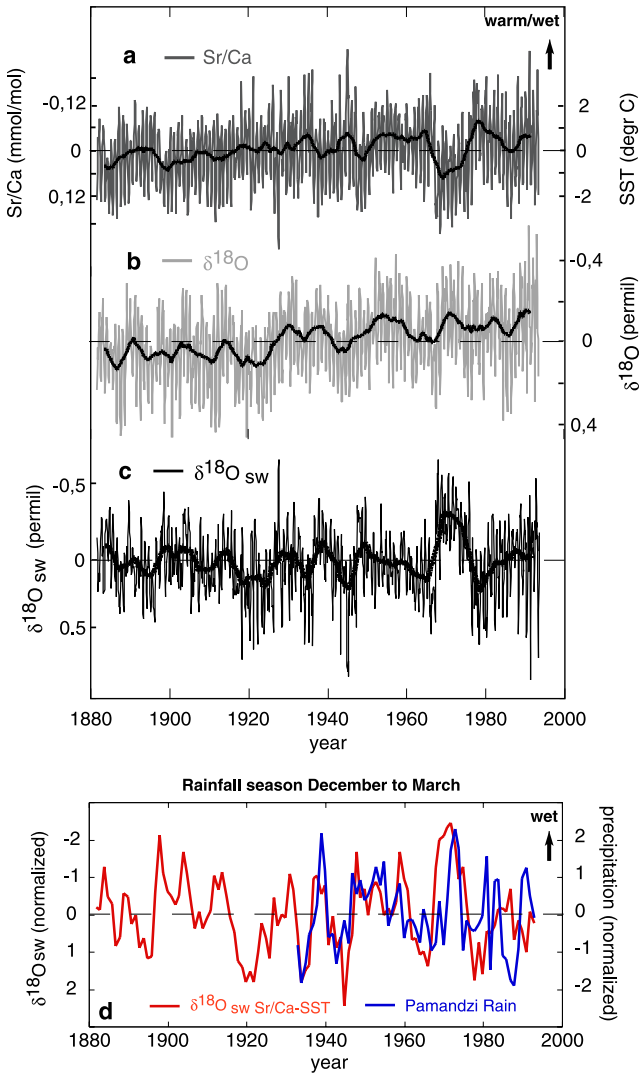

Figure 3. Coral proxy data for the period 1881 to 1994, shown as anomalies relative to their mean. (a) Sr/Ca, (b) oxygen isotopes and (c) reconstructed $\delta^{18}O_{seawater}$ ($\delta^{18}O_{sw}$; bottom). Sr/Ca has been scaled so that −0.058 mmol/mol corresponds to 1°C (see 4.1. for discussion). Bold lines indicate 11-year running mean. (d) Comparison of reconstructed $\delta^{18}O_{seawater}$ ($\delta^{18}O_{sw}$; in red) for the main rainfall season (December to March) with local rainfall from the Mayotte weather station (in blue). Both time series were detrended and normalized.

28.16°C between 1951–1961, and 28.06°C between 1975 and 1998). Assuming a local thermodynamic relationship between SST and atmospheric convection over Mayotte, we would expect mean SSTs > 28°C to be associated with increased convection and a more positive freshwater balance [*Timm et al.*, 2005, and references therein]. However, the reverse is the case. This implies that remotely forced, large-scale atmospheric variability influences the hydrological balance at Mayotte (see 4.3.).

4.3. Large-Scale Climate Teleconnections of $\delta^{18}O_{seawater}$

[18] The instrumental SST and Sr/Ca records of Mayotte are strongly related to ENSO (Figure S7). Here, we use our $\delta^{18}O_{seawater}$ reconstruction as a proxy for changes in the hydrological balance to test for ENSO influences (Table S1 and Figure S2). Correlation maps of seasonal and mean annual values for the period 1950 to 1993 between $\delta^{18}O_{seawater}$ and global SLP show similar, but weaker correlation patterns as with regional-scale rainfall data from the western Indian Ocean south of 10°S (Figures 1a, 1b, and S2) resembling the ENSO SLP pattern. We observe an enrichment of $\delta^{18}O_{seawater}$ in response to ENSO warm events on both seasonal and mean annual scales (Figure S7). This is in contrast to the findings from central Indian Ocean corals (Chagos Archipelago) where $\delta^{18}O$ indicates a positive freshwater balance in response to ENSO warm events over the last 30 years [*Pfeiffer et al.*, 2006]. However, our results agree with earlier studies, in which the western Indian Ocean south of 10°S shows an opposite ENSO response compared to the equatorial Indian Ocean/East Africa [*Hastenrath et al.*, 1993; *Richard et al.*, 2000; *Zinke et al.*, 2004]. The western pole of maximum rainfall anomalies during warm ENSO events is located between 10°S–10°N, 50–70°E which would favor moisture convergence equatorwards of 10°S and a possibly dryer atmosphere to the south [*Neelin et al.*, 2003]. The correlation with the Nino3.4 Index is significantly higher in the period 1975–1994 ($r = 0.61$, $p < 0.006$) than between 1951–1974 ($r = 0.29$, $p < 0.19$; Figure S7). This is consistent with results from the Chagos Archipelago where the ENSO correlation increased after 1975 [*Pfeiffer et al.*, 2006]. However, the El Nino response at Mayotte (drier) and Chagos (wetter) oppose each other. This agrees with the expected rainfall pattern across the Indian Ocean from remote ENSO forcing. Our findings add to the growing evidence of a strengthening of the ENSO signal in Indian Ocean rainfall since 1975 [*Richard et al.*, 2000; *Pfeiffer et al.*, 2006; *Zubair and Ropelewski*, 2006].

[19] The correlation map also indicates high correlations of the instrumental and $\delta^{18}O_{seawater}$ record with the extratropical North and South Pacific SST and SLP resembling the Pacific Decadal Oscillation (PDO) pattern (Figures 1a, 1b, and S2). The PDO is the dominant mode of interdecadal variability in Indo-Pacific SST/SLP [*Deser et al.*, 2004, and references therein]. Mayotte is located in the region of most significant correlations with the PDO [*Deser et al.*, 2004; *Crueger et al.*, 2008]. Linear least squares regression indicates a strong relationship between our $\delta^{18}O_{seawater}$ record and the PDO between 1950–1994 on mean annual and seasonal time scales ($r = 0.6$, $p < 0.003$: Figure S8). The observed periodicity in the $\delta^{18}O_{seawater}$ record ranges between 18–25 years, adding further evidence for an atmospheric bridge between the North Pacific and the Indian Ocean.

5. Conclusions

[20] We developed a 113 year long, bimonthly resolved coral record of $\delta^{18}O_{seawater}$ from Mayotte (south-western Indian Ocean). The $\delta^{18}O_{seawater}$ record indicates that the precipitation-evaporation balance varies on time scales of 5–6 years and 18–25 years. We observe a warm/dry (cool/wet) relationship between SST and $\delta^{18}O_{seawater}$, suggesting that atmospheric variability is remotely forced by large-scale climate anomalies in the Indian Ocean and the

tropical/extratropical Pacific Ocean. The observed interdecadal variability of $\delta^{18}O_{seawater}$ and its spatial signature indicate a possible link to the Pacific Decadal Oscillation, while interannual variability is clearly related to the El Niño-Southern Oscillation. Warm ENSO events are associated with a negative freshwater balance. The ENSO correlation increases after 1975. This agrees with coral data from the Chagos Archipelago (central Indian Ocean) where the ENSO correlation also increased after 1975. However, the El Niño response at Mayotte (drier) and Chagos (wetter) oppose each other. This agrees with the expected rainfall pattern across the Indian Ocean from remote ENSO forcing. Our case study demonstrates that a much denser network of $\delta^{18}O_{seawater}$ reconstructions is crucial for the understanding of spatial patterns in hydrological conditions.

[21] **Acknowledgments.** The coral was drilled by the TESTREEF-group in 1994. Seawater monitoring was carried out by DAF/SPEM Mayotte and F. Seguin. B. Nicet provided the SSTi and SST logger data. Oxygen isotope analysis were carried out at IFM-GEOMAR and the University of Erlangen. B. Schnetger (University of Oldenburg) provided measurement capacity at the ICP-AES. This research was supported by the German Science Foundation and by the German government (KIHZ). We acknowledge the Nederlandse Organisatie voor Wetenschappelijk Onderzoek (NWO-ALW grant 854.00.034 to Jens Zinke). OT was supported by the Japan Agency for Marine-Earth Science and Technology (JAMSTEC) through its sponsorship of the International Pacific Research Center. MP was sponsored by the DFG (grant PF 676/1). CD was supported by the DFG (Leibniz award). This is IPRC publication 552 and SOEST publication 7565.

References

Allan, R. J., and T. J. Ansell (2007), A new globally complete monthly historical mean sea level pressure data set (HadSLP2), 1850–2004, *J. Clim.*, *19*, 5816–5842.

Annamalai, H., J. M. Slingo, K. R. Sperber, and K. Hodges (1999), The mean evolution and variability of the Asian summer monsoon: Comparison of the ECMWF and NCEP/NCAR reanalysis, *Mon. Weather Rev.*, *127*, 1157–1186.

Annamalai, H., K. Hamilton, and K. R. Sperber (2007), South Asian summer monsoon and its relationship with ENSO in the IPCC AR4 Simulations, *J. Clim.*, *20*, 1071–1092.

Cahyarini, S. Y., M. Pfeiffer, O. Timm, W.-C. Dullo, and D. Garbe-Schoenberg (2008), Reconstructing seawater $\delta^{18}O$ from paired coral $\delta^{18}O$ and Sr/Ca ratios: Methods, error analysis and problems, with examples from Tahiti (French Polynesia) and Timor (Indonesia), *Geochim. Cosmochim. Acta*, *72*, 2841–2853.

Charles, C. D., D. E. Hunter, and R. G. Fairbanks (1997), Interaction between the ENSO and the Asian monsoon in a coral record of tropical climate, *Science*, *277*, 925–928.

Cole, J. E., R. B. Dunbar, T. R. McClanahan, and N. A. Muthiga (2000), Tropical Pacific forcing of decadal SST variability in the western Indian Ocean over the past two centuries, *Science*, *287*, 617–619.

Corrége, T. (2006), Sea surface temperature and salinity reconstructions from coral geochemical tracers, *Palaeogeogr. Palaeoclimatol. Palaeoecol.*, *232, 408–428.*

Crueger, T., J. Zinke, and M. Pfeiffer (2008), Dominant Pacific SLP and SST variability recorded in Indian Ocean corals, *Int. J. Earth Sci.*, doi:10.1007/s00531-008-0324-1.

Dansgaard, W. (1964), Stable isotopes in precipitation, *Tellus*, *16*, 436–468.

Deser, C., A. S. Phillips, and J. W. Hurrell (2004), Pacific interdecadal climate variability: Linkages between the tropics and the North Pacific during boreal winter since 1900, *J. Clim.*, *17*, 3109–3124.

Hastenrath, S., A. Nicklis, and L. Greischar (1993), Atmospheric-hydrospheric mechanisms of climate anomalies in the western equatorial Indian Ocean, *J. Geophys. Res.*, *98*, 20,219–20,235.

Juillet-Leclerc, A., and G. Schmidt (2001), A calibration of the oxygen isotope paleothermometer of coral aragonite from *Porites*, *Geophys. Res. Lett.*, *28*, 4135–4138.

Kalnay, E., et al. (1996), The NCEP/NCAR 40-year reanalysis project, *Bull. Am. Meteorol. Soc.*, *77*, 437–471.

Kumar, A., F. Yang, L. Goddard, and S. Schubert (2004), Differing trends in the tropical surface temperatures and precipitation over land and oceans, *J. Clim.*, *17*, 644–653.

Lapègue, J. (1999), Aspects quantitatifs et qualitatifs de la Pluviometrie dans deux enjeux majeurs de la problemtique de l'eau a Mayotte: La Ressource hydrique, l'assainissement pluvial et l'erosion, Ph.D. thesis, 377 pp., Univ. de La Réunion, Saint-Denis, France.

Neelin, J. D., C. Chou, and H. Su (2003), Tropical drought regions in global warming and El Niño teleconnections, *Geophys. Res. Lett.*, *30*(24), 2275, doi:10.1029/2003GL018625.

Pfeiffer, M., O. Timm, W.-C. Dullo, and D. Garbe-Schoenberg (2006), Paired coral Sr/Ca and $\delta^{18}O$ records from the Chagos Archipelago: Late twentieth century warming affects rainfall variability in the tropical Indian Ocean, *Geology*, *34*(12), 1069–1072.

Richard, Y., S. Trzaska, P. Roucou, and M. Rouault (2000), Modification of the southern African rainfall variability/ENSO relationship since the late 1960's, *Clim. Dyn.*, *16*, 883–895.

Reynolds, R. W., N. A. Rayner, T. M. Smith, D. C. Stokes, and W. Q. Wang (2002), An improved in situ and satellite SST analysis for climate, *J. Clim.*, *15*, 1609–1625.

Timm, O., M. Pfeiffer, and W.-C. Dullo (2005), Nonstationary ENSO-precipitation teleconnection over the equatorial Indian Ocean documented in a coral from the Chagos Archipelago, *Geophys. Res. Lett.*, *32*, L02701, doi:10.1029/2004GL021738.

Zinke, J., W.-C. Dullo, G. A. Heiss, and A. Eisenhauer (2004), ENSO and Indian Ocean subtropical dipole variability is recorded in a coral record off southwest Madagascar for the period 1659–1995, *Earth Planet. Sci. Lett.*, *228*(1–2), 177–194.

Zinke, J., M. Pfeiffer, O. Timm, W.-C. Dullo, and G. R. Davies (2005), Atmosphere-ocean dynamics in the western Indian Ocean recorded in corals, *Philos. Trans. R. Soc., Ser. A*, *363*, 121–142.

Zubair, L., and C. F. Ropelewski (2006), The strengthening relationship of ENSO and the northeast Monsoon rainfall over Sri Lanka and Southern India, *J. Clim.*, *19*, 1567–1575.

W.-C. Dullo, Department of Ocean Circulation and Climate, Leibniz Institut fuer Meereswissenschaften, IFM-GEOMAR, Wischhofstrasse 1-3, D-24148 Kiel, Germany.

D. Kroon, School of GeoSciences, University of Edinburgh, West Mains Road, Edinburgh EH9 3JW, UK.

M. Pfeiffer, Institut für Geologie und Mineralogie, Universität zu Köln, Zülpicher Str. 49a/b, D-50674 Köln, Germany.

B. A. Thomassin, Station marine d'Endoume, Centre d'Oceanology Marseille, Chemin de la batterie des Lions, F-13007 Marseille CEDEX, France.

O. Timm, IPRC, SOEST, University of Hawaii, POST Building 413, 1680 East West Road, Honolulu, HI 96822, USA.

J. Zinke, Paleoclimatology and Geomorphology, Vrije Universiteit Amsterdam, De Boelelaan 1085, NL-1081 HV Amsterdam, Netherlands. (jens.zinke@falw.vu.nl)